Autumn upwelling in the Alaskan Beaufort Sea influences gray whale call occurrence

Robert S. Pickart[1], Daniel J. Torres[1], Carin J. Ashjian[1], and Sue E. Moore[2]

Submitted to Deep-Sea Research II, May 2017

Corresponding Author: R. Pickart (rpickart@whoi.edu)

[1]Woods Hole Oceanographic Institution; Woods Hole, MA, USA.

[2]Office of Science and Technology, NOAA/Fisheries, Seattle, WA, USA

Abstract

The relationship between wind-driven upwelling and the occurrence of gray whale calls is explored using data from a mooring array deployed across the shelfbreak and slope of the Alaskan Beaufort Sea together with nearby passive acoustic records. The target strength derived from the acoustic Doppler current meters on the moorings is used as a proxy for zooplankton abundance. In autumn the zooplankton diurnal signal is maximized at a depth of 30-40 m where a sharp density interface resides at the base of the mixed layer, presumably trapping the phytoplankton there. Under enhanced easterly winds, the shelfbreak jet reverses and the secondary circulation fluxes zooplankton onto the shelf. At the conclusion of the wind events an eastward-flowing "rebound jet" is temporarily established. Gray whale call detections were greatest during times when the rebound jet was present and upwelled water resided on the outer shelf and upper slope, implying that the whales respond to the introduction of prey onto the shelf. Individual peaks in gray whale call occurrence were generally associated with enhanced target strength, except during times of full ice cover which likely prohibited the whales from accessing the region. Our results suggest an important predator-prey relationship for gray whales and zooplankton associated with autumn upwelling on the Beaufort slope.

Keywords: Arctic Ocean, boundary currents, upwelling, gray whales

1. Introduction

Upwelling in the Alaskan Beaufort Sea occurs during all seasons and under varied ice conditions (Schulze and Pickart, 2012; Lin et al., 2016). Driven by enhanced easterly winds, the Ekman transport fluxes water offshore in the surface layer, while the return flow at depth pulls water from the basin onto the shelf. This can result in a substantial exchange of heat, freshwater, inorganic nutrients, and carbon across the shelfbreak (e.g. Mathis et al., 2012; Pickart et al., 2013a). The atmospheric forcing is due to the combined action of the Beaufort High and Aleutian Low. Typically, an upwelling event is triggered by a passing low-pressure system to the south, in conjunction with a strengthening of the Beaufort High (Pickart et al., 2009; Mathis et al., 2012; Pickart et al., 2013b). The presence of pack-ice modulates the oceanographic response. For a given wind speed, the upwelling is strongest when there is partial ice cover and weakest when the concentration is near 100% (as long as the ice is mobile, Schulze and Pickart, 2012). The open water response is intermediate to these two cases.

The prevailing winds in the Alaskan Beaufort Sea are from the east. Seasonally they are strongest in the early-summer and mid-fall (Pickart et al., 2013b), and, consequently, the upwelling is strongest during these times (Lin et al., 2016). Using mooring data and weather station wind records, Lin et al. (this issue) found a statistically significant relationship between the cumulative Ekman transport and an upwelling index based on the potential density anomaly near the shelfbreak. Notably, however, wind strength does not seem to be the primary factor governing the upwelling of Atlantic water, which resides in the lower halocline in the Canada Basin. Instead, the seasonal change in the wind stress curl offshore of the boundary dictates the ability for this deep water to be brought to the shelf. During the cold months of the year the halocline is displaced upwards by the positive wind stress curl, which makes the Atlantic layer more accessible for upwelling.

A typical upwelling event along the Beaufort slope unfolds as follows (see Pickart et al., (2013a) and Lin et al. (this issue) for details). Shortly after the easterly winds increase, the shelfbreak jet reverses direction and flows to the west as a surface-intensified current, typically flowing around 20 cm s^{-1}, but at times reaching speeds up to 100 cm s^{-1}. Roughly 10 hours later the upwelling commences, advecting water from the basin onto the shelf. Then, before the winds completely subside, an eastward-flowing "rebound jet" is established due to the alongstream pressure gradient force. This jet has a deep-reaching tail extending into the Atlantic water that lasts for several days, after which only the shelfbreak portion remains (i.e. the normal eastward-flowing shelfbreak jet). The rebound jet is a ubiquitous feature of upwelling on the Beaufort slope, and, since upwelling is so common, its signature appears in a year-long mean section of velocity. The frequent occurrence of the rebound jet led Aagaard (1984) to call this feature the Beaufort undercurrent.

Through the course of the year, the Beaufort shelfbreak jet advects Pacific water eastward from Barrow Canyon (Nikolopoulos et al., 2009; see Fig. 1). The jet is narrow (10-15 km wide) and has a mean transport of order 0.1 Sv. During summertime it is surface-intensified and carries mostly Pacific summer waters, while over the remainder of the year it is bottom intensified and advects primarily Pacific winter waters (Nikolopoulos et al., 2009; Brugler et al., 2014). At the end of the winter season, much (if not all) of the Chukchi Sea is filled with newly ventilated, nutrient-rich winter water (Pacini et al., this issue). This is the result of input from the Bering Sea, as well as local convection on the Chukchi shelf (when leads and polynyas open up) that stirs up remineralized nutrients from the bottom. Consequently, just as the phytoplankton growing season commences, the shelfbreak jet is supplying nutrients to the Beaufort Sea. As such, the current influences the regional ecosystem, including the carbon budget of the western Arctic Ocean. Importantly, the remnant (older) winter water is also relatively high in nitrate and silicate. The shelfbreak jet thus transports nutrients year-round. This is true even in summer when there is remnant winter water immediately below the Pacific summer water.

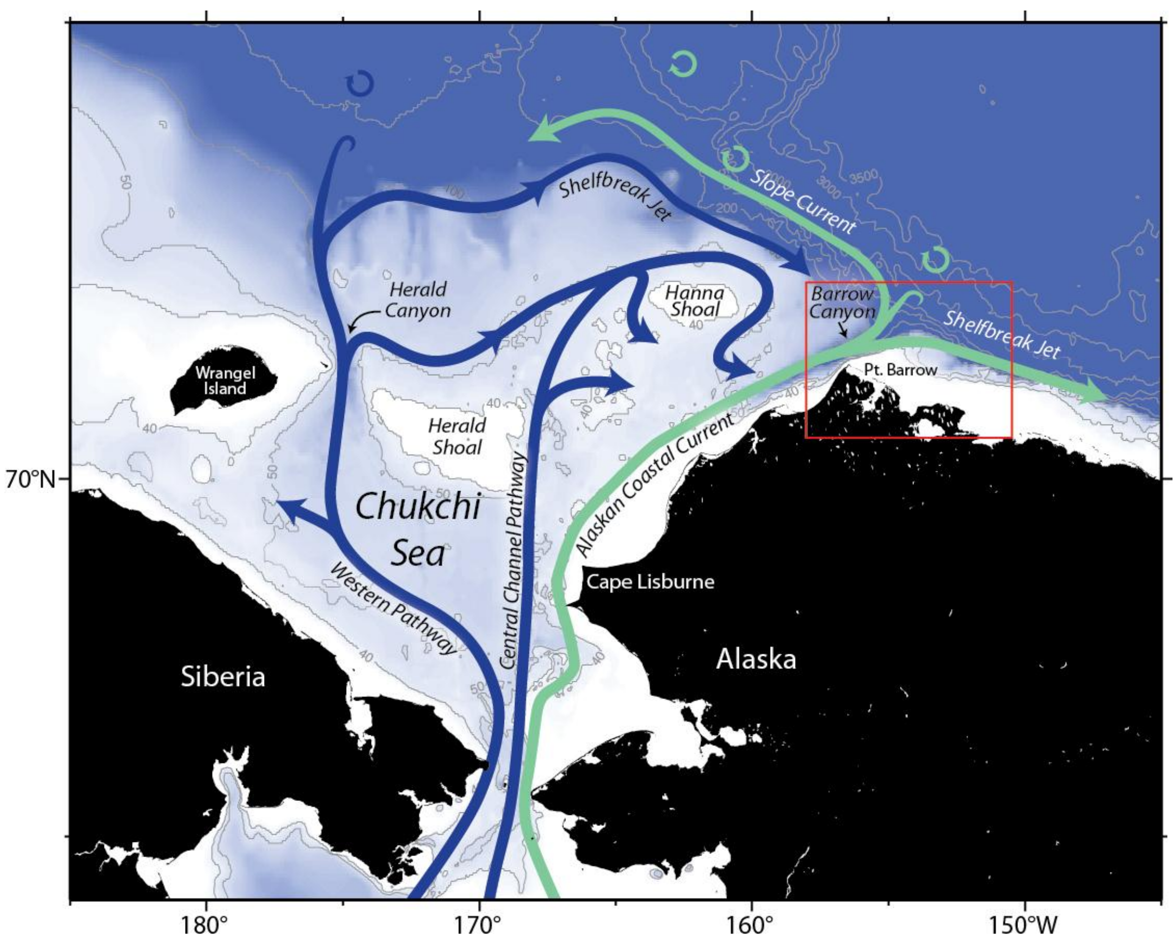

Figure 1: Schematic circulation of the Chukchi and western Beaufort Seas, after Corlett and Pickart (2017). The red box outlines the study domain shown in detail in Fig. 2.

A mix of small, shelf-type zooplankton species (e.g., *Pseudocalanus* spp.) and larger, slope-basin type species are found on the Beaufort shelf and shelfbreak. In particular, the large copepods *Calanus hyperboreus* and *C. glacialis* that dominate the biomass in the Arctic Basin (see Ashjian et al., 2003; Hopcroft et al., 2005) are present during summer along the shelfbreak and farther inshore on the Beaufort shelf (Lane et al., 2006; Llinas et al., 2009; Smoot and Hopcroft, 2017b). These species overwinter obligately at depth in the Arctic Basin (e.g., Ashjian et al., 2003; Falk-Petersen et al., 2009) and likely descend to those depths in late summer and early fall. Euphausiids, potentially originating from the Bering Sea, also can be found below the pycnocline along the shelfbreak (Ashjian et al., 2010; Smoot and Hopcroft, 2017a), presumably advected there by the Beaufort shelfbreak jet. The elevated levels of phytoplankton in the jet are thought to provide an aggregation point for zooplankton feeding (e.g., Ashjian et al., 2005; Lane et al., 2008; Smoot and Hopcroft, 2017a).

Wind-driven upwelling may be particularly important to zooplankton distribution and composition on the Beaufort Shelf, bringing the large *Calanus* spp. and euphausiids from depth onto the shelf. Another mesoscale process impacting the transport of zooplankton is eddy formation from the shelfbreak jet. Since the jet is baroclinically unstable (Spall et al., 2008; von Appen and Pickart, 2012) it regularly spawns eddies that propagate into the Canada Basin. Llinas et al. (2009) found elevated concentrations of zooplankton, including species of both Pacific Water and Arctic basin origin, within one such cold-core eddy. They hypothesized that the Arctic species had been upwelled onto the shelf to co-mingle with the Pacific species in the shelfbreak jet prior to the formation of the eddy. Presently it is unknown how these two mechanisms – wind forcing and eddy formation – compare in efficiency, and what the net flux of zooplankton is due to such mesoscale activity.

Three species of cetaceans – bowheads, belugas, and gray whales – migrate in the spring from the Bering Sea to the Chukchi / Beaufort Seas in search of prey, returning south again in the fall. These are the only cetaceans to inhabit the western Arctic in significant numbers. Habitat selection is species-specific and varies seasonally (Moore et al., 2000; Clarke et al., 2016; Stafford et al., 2013; Hauser et al. 2017). In the northeastern Chukchi Sea, gray whales select shallow (<35 m) coastal habitat in summer and shelf/trough (50-200m) habitat in fall (Clarke et al., 2016), with whale distribution often extending into the western Beaufort Sea.

Gray whales are capable of straining prey both from the water column and from epi- and infaunal benthic communities (Nerini, 1984). It is becoming evident that the Beaufort shelfbreak jet plays a central role in the patterns and availability of this prey. For example, large aggregations of bowheads have been observed near areas of upwelling in the western Beaufort Sea during late summer (Ashjian et al. 2010; Moore et al. 2010; Okkonen et al. 2011, 2017). It has been demonstrated that the timing of the fall migration of bowheads and belugas along the Beaufort slope coincides with the autumn peak in shelfbreak upwelling (Lin et al, 2016). Using passive acoustic data from the Beaufort slope, Stafford et al. (2007) found that gray whales were present not only through the fall but into the winter season. It remains to be determined what factors allow these whales to remain so late into the year. Stafford et al. (2007) noted that decreasing ice concentrations due to the warming climate are now resulting in open water pathways for the whales in late-autumn and winter, but the question of prey availability still remains open.

This paper uses oceanographic mooring timeseries in conjunction with contemporaneous passive acoustic data to explore the links between upwelling on the Alaskan Beaufort slope and the occurrence of gray whales in the late-fall and early-winter. We find that there is a causal relationship between the shoreward flux of zooplankton due to the upwelling and the frequency of gray whale calls. We further consider the influence of ice cover in this relationship. The passive acoustic data were collected in fall/winter 2003-4, but we use additional oceanographic mooring data to elucidate the processes involved. We begin with a description of the in-situ data, and then discuss the characteristics of the regional hydrography and circulation in the absence of wind forcing. Different aspects of the upwelling are described next, including the associated flux of zooplankton. Finally, we compare the oceanographic data to the cetacean call data in an effort to identify how the upwelling might impact the feeding patterns of the gray whales.

2. Data and Methods

Physical variables

From August 2002 to September 2004 a mooring array was maintained across the shelfbreak and slope of the Alaskan Beaufort Sea near 152ºW, roughly 150 km to the east of Barrow Canyon (Fig. 2). This was part of the Western Arctic Shelf-Basin Interactions (SBI) program. The array consisted of 8 moorings spanning from the outer-shelf to roughly the 1400 m isobath on the continental slope (Fig. 3). The inshore-most site contained a bottom tripod, and the rest of the sites consisted of tall moorings. For the hydrographic measurements, the tall moorings employed conductivity-temperature-depth (CTD) profilers nominally sampling 2-4 times daily, and the bottom tripod had a MicroCat CTD sensor sampling hourly. For velocity, the inshore 6 moorings had bottom-mounted, upward-facing acoustic Doppler current profilers (ADCPs, either 300 KHz or 75 KHz sampling hourly), and the outer two moorings had an acoustic travel-time current meter on the CTD profiler. The reader is referred to Spall et al. (2008) and Nikolopoulos et al. (2009) for a description of the data processing and sensor accuracies.

Vertical sections of the mooring hydrographic variables (potential temperature, salinity, potential density) and velocity were constructed using Laplacian-Spline interpolation, resulting in 2-4 hydrographic sections per day and 24 velocity sections per day. The velocities were first de-tided using the T_Tide harmonic analysis software package (Pawlowicz et al., 2002). Subsequently, we computed alongstream and cross-stream velocities following Nikolopoulos et al. (2009), where the positive alongstream direction is oriented at 125ºT and the positive cross-stream direction is 35ºT. This rotated coordinate system was determined by considering the angle of the principal axis of variance ellipses at the different sites as well as the direction of the mean flow vectors.

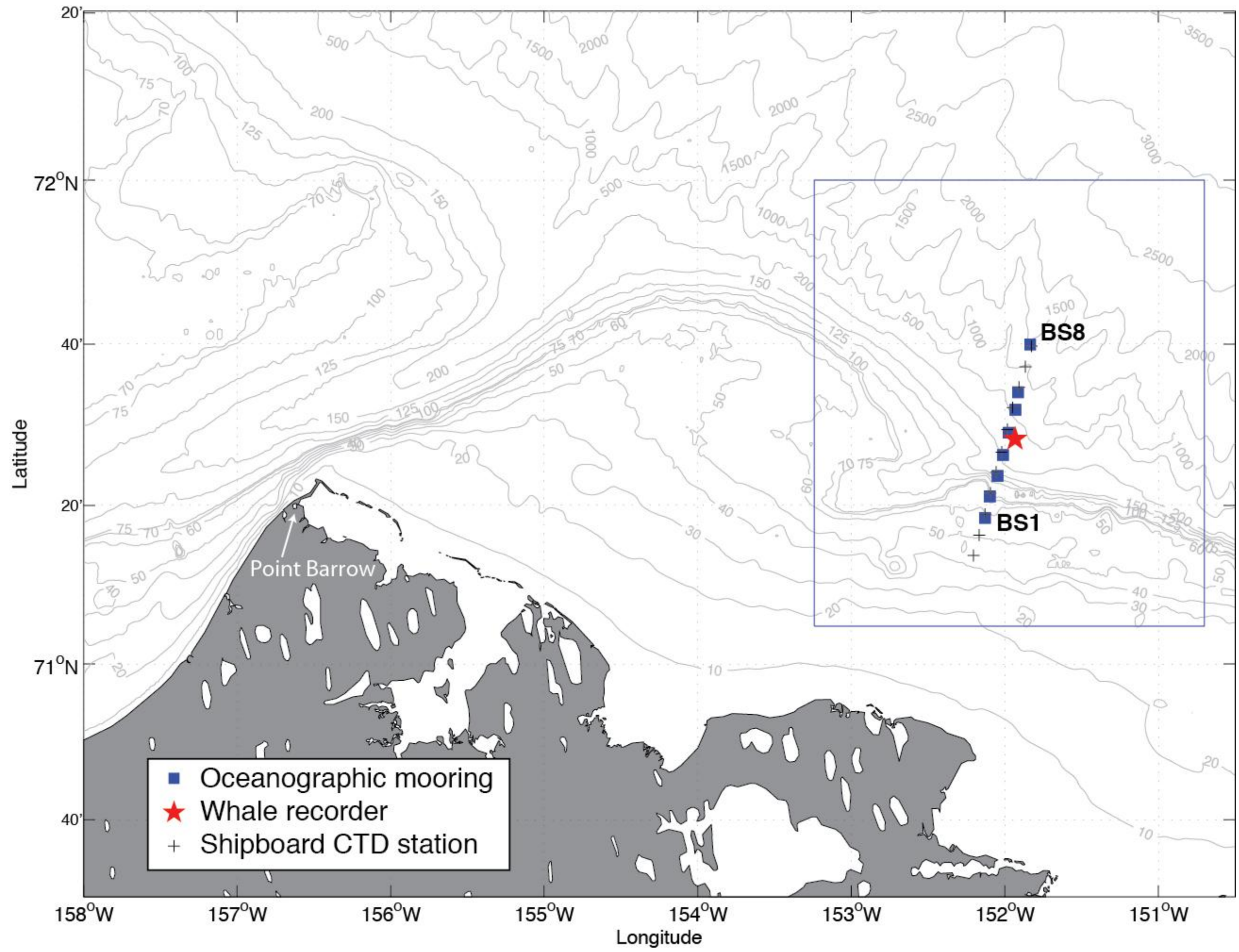

Figure 2: Map of the study region and the data sources (see the legend). The box delimits the region of the ice analysis in Section 5. The bottom topography is IBCAO v3.

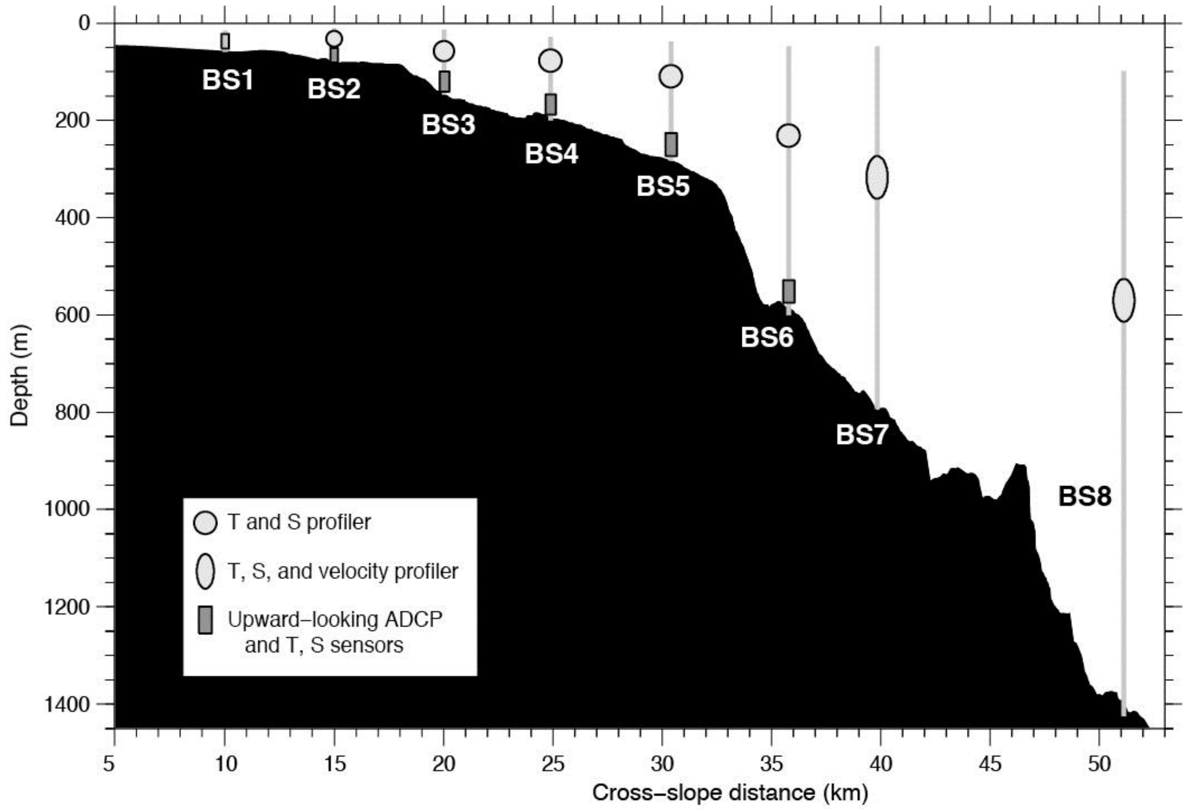

Figure 3: Cross-section view of the SBI Beaufort slope mooring array. The legend shows the type of instrumentation used. The bottom topography is from a shipboard echosounder. The shelfbreak is between moorings BS2 and BS3.

Shipboard hydrographic data from a transect occupied along the mooring line are also used in the study (Fig. 2). The section was carried out from 8-9 October 2003 aboard the USCGC *Healy* (during a turnaround of the mooring array). A 911+ CTD was used on a 24-position rosette with 10 liter Niskin bottles. The temperature sensors underwent laboratory calibrations before and after the field season, and the accuracies were deemed to be 0.001^{o}C. The conductivity sensors were calibrated using the in-situ water sample salinity data. Only bottles deeper than 300 m were used to reduce the scatter. The resulting accuracy of the salinity measurements was estimated to be 0.002. As was done using the mooring data, vertical sections of the shipboard hydrographic variables were constructed using Laplacian-Spline interpolation. In addition to the standard variables, we computed the planetary potential vorticity, $f/\rho(d\rho/dz)$, as a measure of the stratification of the water column, where f is the Coriolis parameter, ρ is density, and z is depth.

The wind data used in our analysis come from the Barrow meteorological station (see Fig. 2). This is located roughly 150 km to the west of the SBI mooring array, but previous studies have demonstrated that the data are indicative of the winds in the vicinity of the array (e.g. Pickart et al., 2011). The Barrow data have been quality controlled and small gaps in the record have been filled using linear interpolation (see Pickart et al., 2013b for details). We use the component of wind in the alongcoast direction (Nikolopoulos et al., 2009), and the wind stress was computed following Large and Pond (1981). The ice concentration data are from the passive radiometer on the Advanced Microwave Scanning Radiometer-Earth Observing System (AMSR-E). This is a daily product with a spatial resolution of 12.5 km and accuracy of 10% (Spreen et al., 2008).

Relative Acoustic Backscatter as a Proxy for Zooplankton

The backscatter data from the ADCPs were used as a proxy for zooplankton abundance. Moored ADCP backscatter data have been used to demonstrate patterns in zooplankton distribution and seasonal changes at a number of locations in the Arctic Ocean (e.g., Cottier et al., 2006; Berg et al., 2008; Hamilton et al. 2013). Although the instruments are not absolutely calibrated and frequently not validated with coincident net data, the relative backscatter can be used to discern diel patterns in vertical distribution and changes in relative backscatter associated with physical events such as upwelling. The data provide only a relative measure of zooplankton abundance, yet when considered within the records of a single instrument during a single deployment they can indicate greater or lesser concentrations of scatterers, here argued to be zooplankton.

As part of the instrument configuration, ADCPs process the return echo at discrete time intervals pertaining to depth cells (or bins) along the range of the ADCP signal (range gating). In addition to measuring the Doppler shift of the transmitted signal to determine the velocity of the water column, ADCPs also record the strength of the return signal (echo intensity) at each depth cell. The strength of the return echo generally decreases as a function of distance from the transducer due to sound absorption and attenuation due to beam spreading. To counteract this, a frequency-dependent absorption coefficient (Urick, 1983) is applied for each instrument, along with an attenuation factor, to calculate target strength (Visbeck, 2002). Since target strength does not inherently decrease with distance from the transducer, it represents a more accurate estimation of the relative backscatter in the water column due to zooplankton concentration. We note that the units of target strength are arbitrary for each instrument. Therefore, it is not meaningful to construct vertical sections of this quantity.

Here we consider individual records from one of the moorings on which a 300 kHz ADCP was used. This frequency should be able to scatter off of, and thus detect, zooplankton of the size of the large copepods and euphausiids thought to be upwelled along the Beaufort shelfbreak (e.g. Llinas et al., 2009; Smoot and Hopcroft, 2017 a and b). These animals are strong diel vertical migrators when a diurnal light cycle is present and, for *Calanus* spp., if overwintering diapause has not commenced (e.g., Coyle and Pinchuk, 2002; Falk-Petersen et al., 2008, 2009). The presence of a diel signal in the vertical distribution of backscatter from the ADCP would be compelling evidence for the signal as a proxy for such zooplankton.

Passive acoustic whale data

During the 2003-4 deployment of the SBI Beaufort slope array, three Acoustic Recording Packages (ARPs) were placed near the mooring line in order to collect information about marine mammals in this region over the course of the year (Stafford et al. 2007). Here we consider the data from the shoreward-most ARP which was positioned at the 318 m isobath (Fig. 2). This instrument is best suited for investigating gray whale occurrence, since these cetaceans commonly reside on the shelf and in the vicinity of the shelfbreak. A second ARP was placed at the 1258 m isobath (not used in this study), and a third instrument was lost.

The ARP is a short mooring with a hydrophone situated roughly 10 m above the seafloor (Wiggins, 2003). The data were collected at 1 KHz and subsequently low-pass filtered (see Stafford et al. (2007) for details). The gray whale calls were then tabulated over 10-min intervals. The parameter used in this study is the ratio of the number of 10-min intervals during which calls were recorded, to the total number of 10-min sampling periods within a day (which varied throughout the deployment). This ratio is referred to as the daily percent gray whale calls and should reflect gray whale occurrence. Unfortunately, the ARP malfunctioned at the end of December 2003. Hence our comparative analysis of gray whale occurrence in relation to the physical environment is limited to the time period from mid-fall to early-winter 2003.

3. Unforced state of the Beaufort shelfbreak jet

In the absence of wind forcing, the Beaufort shelfbreak jet flows to the east centered near the 150 m isobath. It has distinct seasonal configurations (Fig. 4). In the spring it is bottom-intensified and advects primarily Pacific winter water (Fig. 4, top panel). In this state the current is baroclinically unstable and often forms cold-core eddies that populate the southern Canada Basin (Spall et al., 2008; Timmermans et al., 2008). In summer the jet is generally surface-intensified and transports warm Pacific summer waters (Fig. 4, middle panel). This includes Alaskan coastal water, which is advected northward in the Chukchi Sea by the Alaskan coastal current. In this regard the Beaufort shelfbreak jet can be considered the extension of the Alaskan coastal current to the east of Barrow Canyon. However, for a short period in early-summer, and again in the fall, Bering summer water is advected by the shelfbreak jet. When this happens the current is bottom-intensified (see von Appen and Pickart, 2012). The summer mean section of Fig. 4 is dominated by the Alaskan coastal water configuration.

In the winter months the velocity signature of the current is due to a combination of the bottom-intensified shelfbreak jet and the rebound jet discussed in the introduction (Fig. 4, bottom panel). The shelfbreak jet is weakest during this time of year and advects predominantly remnant Pacific winter water, while the rebound jet advects mostly Atlantic water. As noted above, during upwelling events the shelfbreak jet reverses to the west and is surface-intensified. This is reflected in the mean winter velocity of Fig. 4 where the flow in the upper 50 m is westward. The mean winter hydrographic section also reflects the upwelling process: the coldest Pacific winter water is seaward of the velocity core, which is in contrast to the mean spring configuration where the coldest winter water is within the shelfbreak jet. This is because the frequently-upwelled warm Atlantic water moderates the mean temperature on the upper continental slope during winter.

As noted above, the shelfbreak jet advects zooplankton to the east. Here we use the 300 kHz ADCP target strength as a measure of the zooplankton abundance. Due to the fact each ADCP has its own relative value of target strength (which is uncalibrated), it is not meaningful to construct vertical sections of this quantity. However, inspection of the individual records strongly suggests that the target strength is indeed reflective of the zooplankton in the water column at each site because of a strong signal of diel vertical migration of the backscatter. As an example, we show a 3.5-day segment from late-October 2002 from mooring BS2 at the edge of the shelf (Fig. 5).[1] One clearly sees the signature of the diurnal migration of the zooplankton. During the daytime hours, the backscatter/zooplankton abundance is greatest at depth (>55 m), with very low backscatter in the upper 50 m. During the night the backscatter/zooplankton moves upwards into the upper 50 m, with enhanced backscatter in the depth range of 30-40 m. The timing of the upward and downward redistributions of backscatter relate to the times of local sunrise and sunset (indicated in Fig. 5 by the dashed lines). In particular, the upwards movement coordinates closely to sunset while the downwards movement slightly precedes the time of sunrise, perhaps because the animals are satiated or are sensitive to the prolonged twilight period before sunrise. This diel vertical migration is consistent with the known behavior of both euphausiids and non-overwintering *Calanus* spp. copepods.

We quantified the diurnal signal using a multi-taper spectrum analysis of the target strength for the time period October–January for the same mooring. This shows a peak in energy at the 24-hour period at all depth levels (Fig. 6a), with a maximum amplitude between 30-40 m (Fig. 6b). This was also the case for the 3.5-day snapshot in Fig. 5. To elucidate this, we used complex demodulation (e.g. Rosenfeld, 1987) to quantify the time variation of the diurnal amplitude during the three-month time period. In particular, 2-day segments of the timeseries were fit to a sine wave with a 24 hr period, and the segments were shifted by 12 hours over the length of the record. This reveals that the peak in diurnal energy persisted at this depth level until mid-November, after which it descended to deeper depths through the end of December (Fig. 7). The magnitude of the signal also decreased abruptly in early November and became more sporadic later into the fall and early winter. This pattern further suggests that the backscatter serves as a

[1] Because of the near-surface blanking interval and the position of the ADCP just above the sea floor, the ADCP at site BS2 only collected data from 15-60 m of the 83 m deep water column.

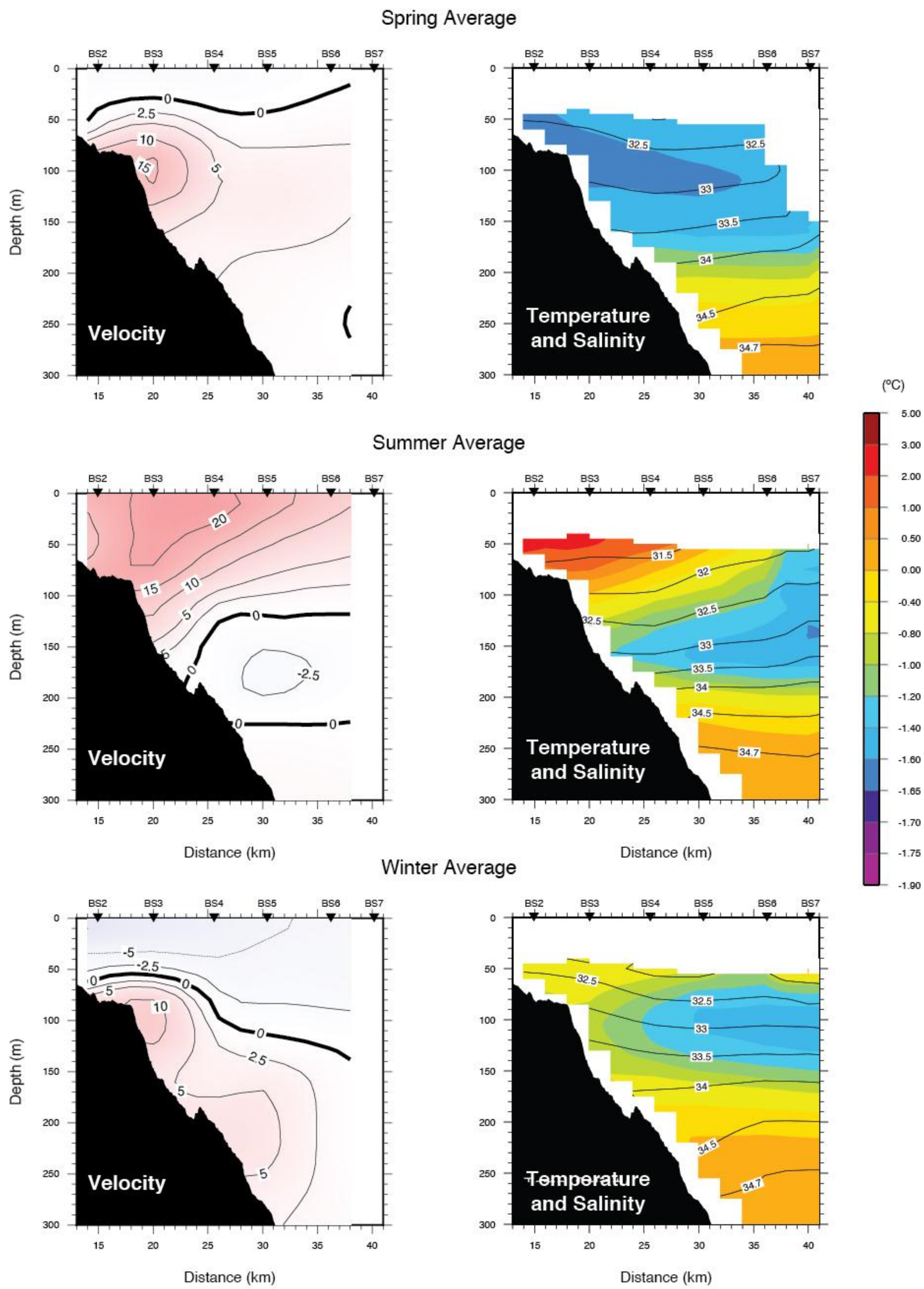

Figure 4: Seasonal mean composite sections calculated using the first year of data from the SBI mooring array. The left-hand column is alongstream velocity (cm s^{-1}, where positive is eastward). The right-hand column is potential temperature (color) overlain by salinity (contours). The mooring locations are indicated along the top. The viewer is looking to the west.

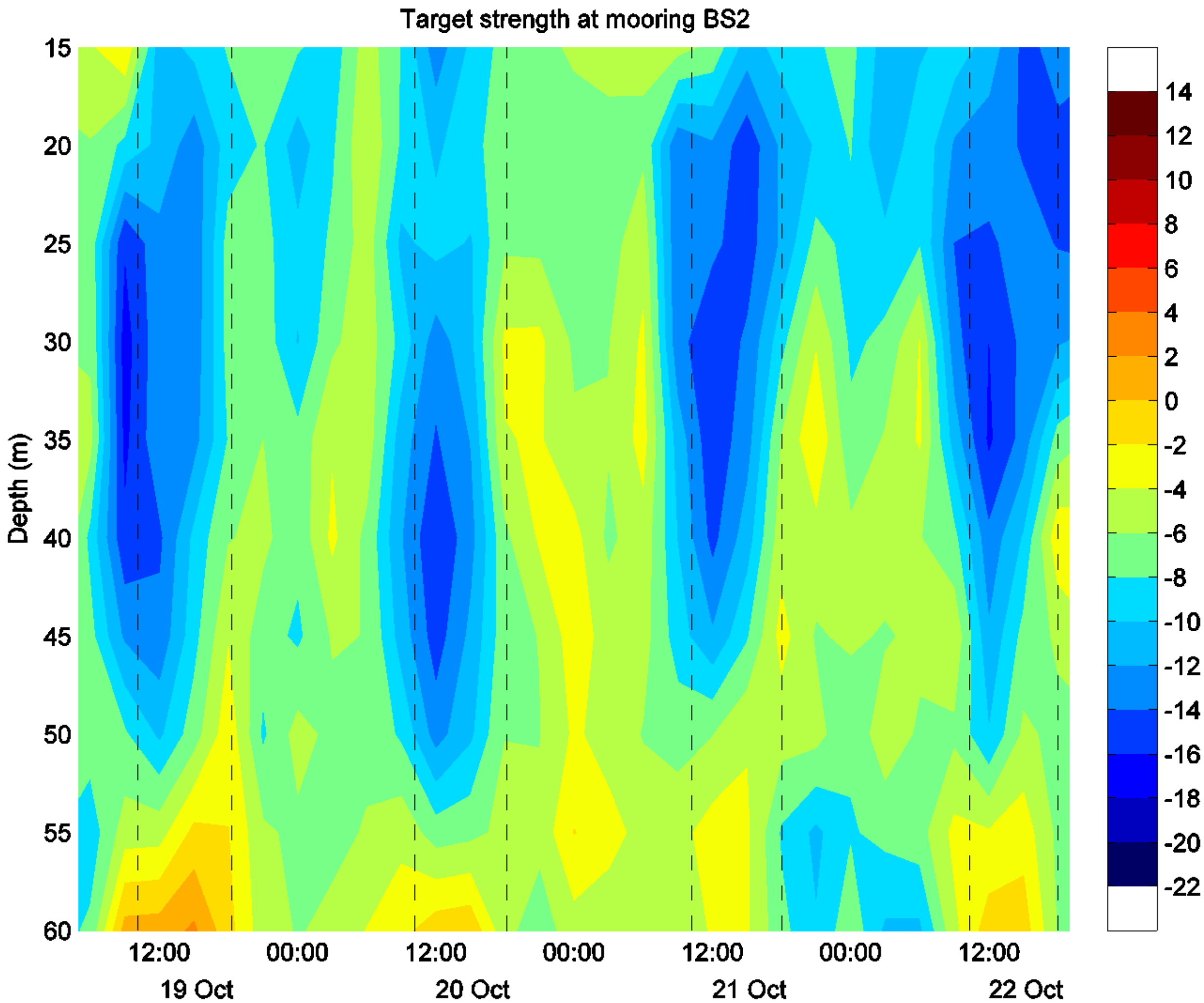

Figure 5: Target strength at mooring BS2 for a 3.5-day period in October 2002. The dashed lines indicate the times of local sunrise and sunset over the period.

useful proxy for the distribution and relative abundance of zooplankton in these data, since the timing of the vertical redistribution follows the expected diel signal and the signal decreases in late fall and winter when daily light signals are diminished and large copepods are in overwintering diapause.

Why is there a peak in diurnal energy at this depth range? Unfortunately, the CTD profilers on the moorings did not sample above 40 m depth (to keep them safe from ridging pack ice), so we cannot discern any information about the hydrographic structure of the water column in the depth range of interest. However, a shipboard CTD section was occupied along the mooring line in early October which provides a likely explanation (Fig. 8). One sees that in early fall the mixed layer was roughly 30 m deep (Fig. 8a), extending from the outer shelf to the offshore edge of the section. Below the mixed layer was a density interface with enhanced stratification. This is seen in the vertical section of planetary potential vorticity, which reveals a region of strong stratification near 30-40 m depth (Fig. 8b). Hence, the zooplankton were likely aggregating at the pycnocline during night to feed on the phytoplankton, microzooplankton, and particulate organic material that should accumulate there.

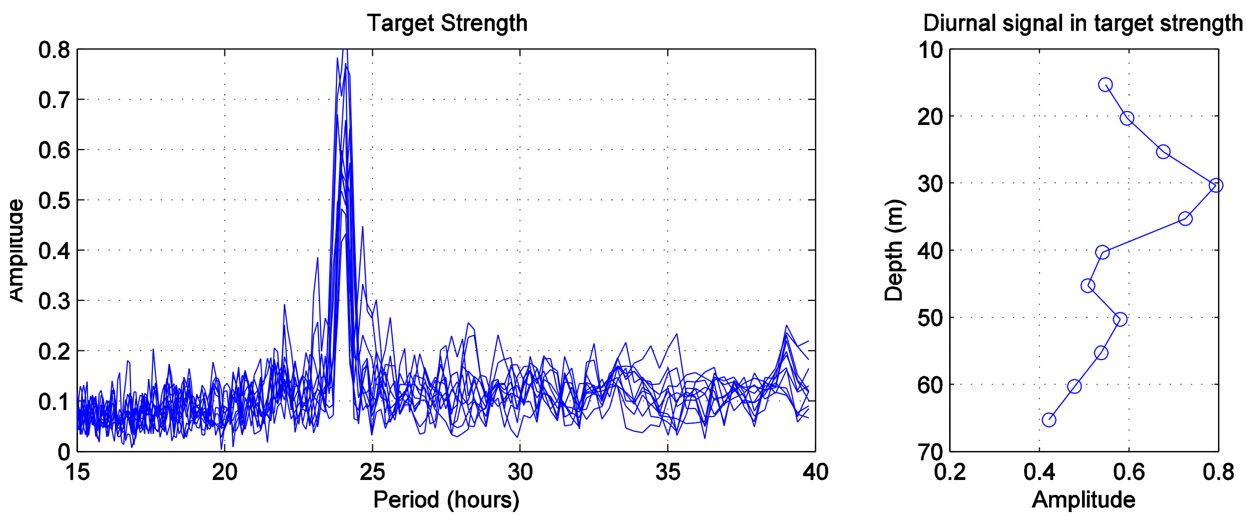

Figure 6: (a) Spectral amplitude of the target strength at mooring BS2 for the period 1 Oct – 31 Dec 2002. (b) Amplitude of the diurnal signal as a function of depth.

Fig. 7 suggests that the mixed layer started to deepen in mid-November, allowing the zooplankton to settle deeper in the water column later in the fall. Interestingly, the sudden decrease in diurnal energy in early November coincided with a strong upwelling event on the Beaufort slope (Pickart et al., 2013a). This apparently altered the presence of zooplankton in the region for the remainder of the year. This could be the result of a large net onshore flux of zooplankton to the inner shelf. Notably, this same storm fluxed a substantial amount of nitrate and dissolved organic carbon onshore, while transporting a large quantity of heat offshore (Pickart et al., 2013a). We now consider the upwelling process and the resulting transport of zooplankton using the mooring data.

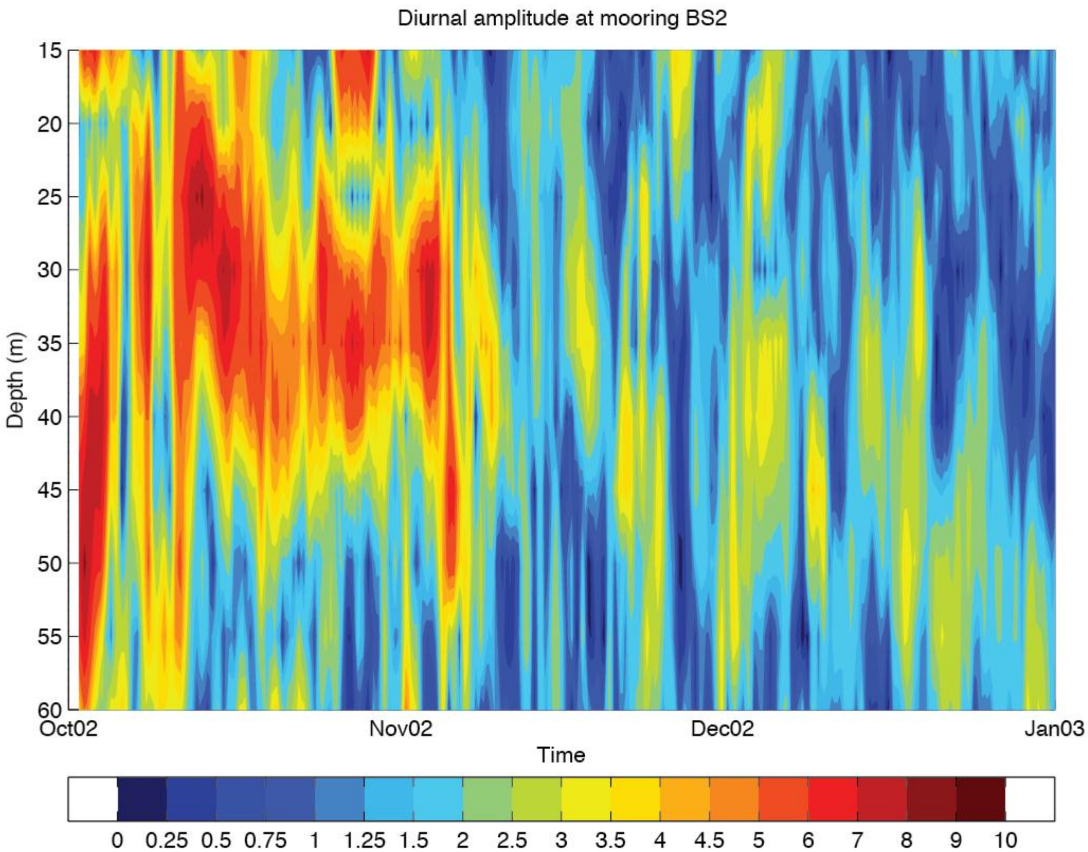

Figure 7: Amplitude of the diurnal signal in target strength at mooring BS2 computed using complex demodulation (see text).

4. Upwelling and zooplankton flux

As described in the introduction, upwelling on the Beaufort slope occurs regularly under enhanced easterly winds. First the shelfbreak jet reverses to the west, followed by shoreward transport of water from the basin to the shelf. Let us examine an individual storm that took place in early November 2002. This is the same storm investigated by Pickart et al. (2011) and Pickart et al. (2013a). It was a strong event that lasted roughly three days, with a peak wind stress of 0.4 N m^{-2} (peak wind speed of 18 m s^{-1}, Fig. 9a). The CTD profiler on mooring BS2 revealed that, shortly after the peak in wind stress, warm and salty Atlantic water appeared at the mooring site (Fig. 9b). This water typically resides in the basin at a depth greater than 150 m (see the offshore

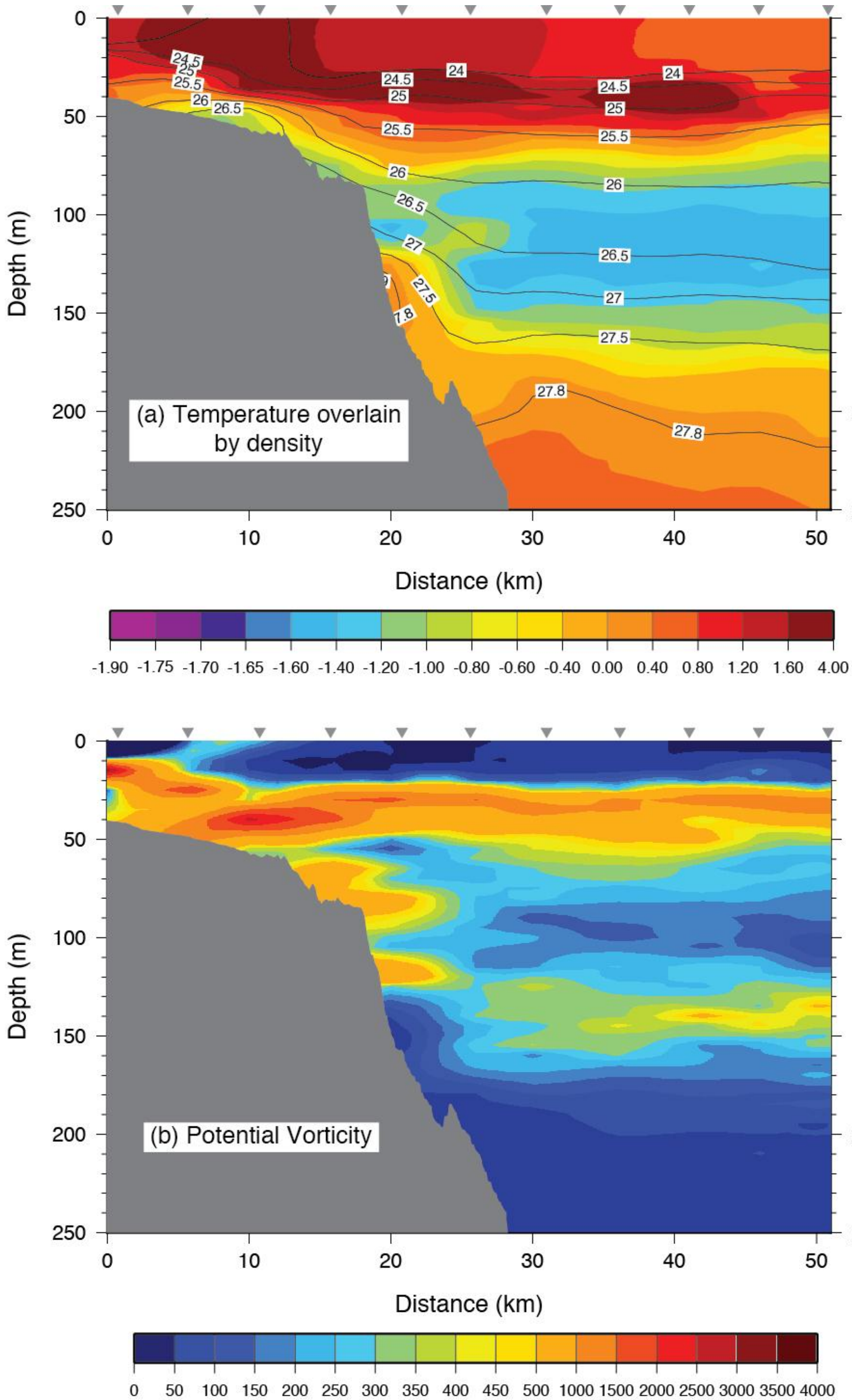

Figure 8: Vertical sections from the shipboard transect occupied in October 2003. (a) Potential temperature (color, ºC) overlain by potential density (contours, kg m^{-3}). (b) Planetary potential vorticity (m^{-1} s^{-1} x 10^{-11}). The CTD station positions are marked along the top.

part of the vertical section in Fig. 8). Hence, during the storm, the water upwelled more than 100 m as it progressed shoreward.

The evolution of the event followed the canonical sequence described in the introduction. Before the onset of the easterly winds the shelfbreak jet was flowing to the east (Fig. 10b), and at the height of the storm it reversed to the west at speeds exceeding 100 cm s^{-1}. As the winds subsided the eastward-flowing rebound jet spun up, the upper portion of which was sampled by the BS2 mooring (Fig. 10b). The secondary circulation consisted of an Ekman cell, with offshore transport in the upper 30 m and onshore transport deeper than this (Fig. 10c). The target strength calculated from the ADCP is shown in Fig. 10d. This demonstrates clearly that the onshore flow advected a large amount of zooplankton onto the shelf during the event (note the strong diurnal signal preceding the upwelling event, potentially caused by euphausiids). The zooplankton were resident in the Atlantic layer of the basin prior to the storm (verified by the offshore mooring data). Hence, the upwelling event may have tapped zooplankton that had begun the overwintering process, with weak or non-existent diel vertical migration, making them available as prey for gray whales.

5. Relationship to gray whale occurrence

The ARPs that were deployed next to the SBI mooring array in 2003 were the first such passive acoustic devices deployed in the Alaskan Beaufort Sea, and revealed that gray whales are present in this region through the fall and winter months (Stafford et al., 2007). The daily percent occurrence of the gray whales at the ARP site on the upper continental slope (Fig. 2) displays pronounced variability through the record, with values ranging from 0 to 100% (Fig. 11). We now investigate if the cetaceans responded to the introduction of prey onto the shelf due to upwelling activity.

In an effort to identify patterns, we constructed two composites of the physical data. The first composite is for those periods when the percent gray whale occurrence was less than 15%, and the second is for times when it exceeded 50% (results are not sensitive to the precise choices of these criteria). As seen in Fig. 12a, gray whales were relatively scarce when the shelfbreak jet was in its normal configuration for this time of year, i.e. a bottom-intensified current trapped to the shelfbreak. By contrast, the whales were prevalent in this region when the rebound jet was well developed (Fig. 12b). As discussed above, this configuration corresponds to the end of an upwelling event after the zooplankton have been fluxed onto the shelf. This is precisely what

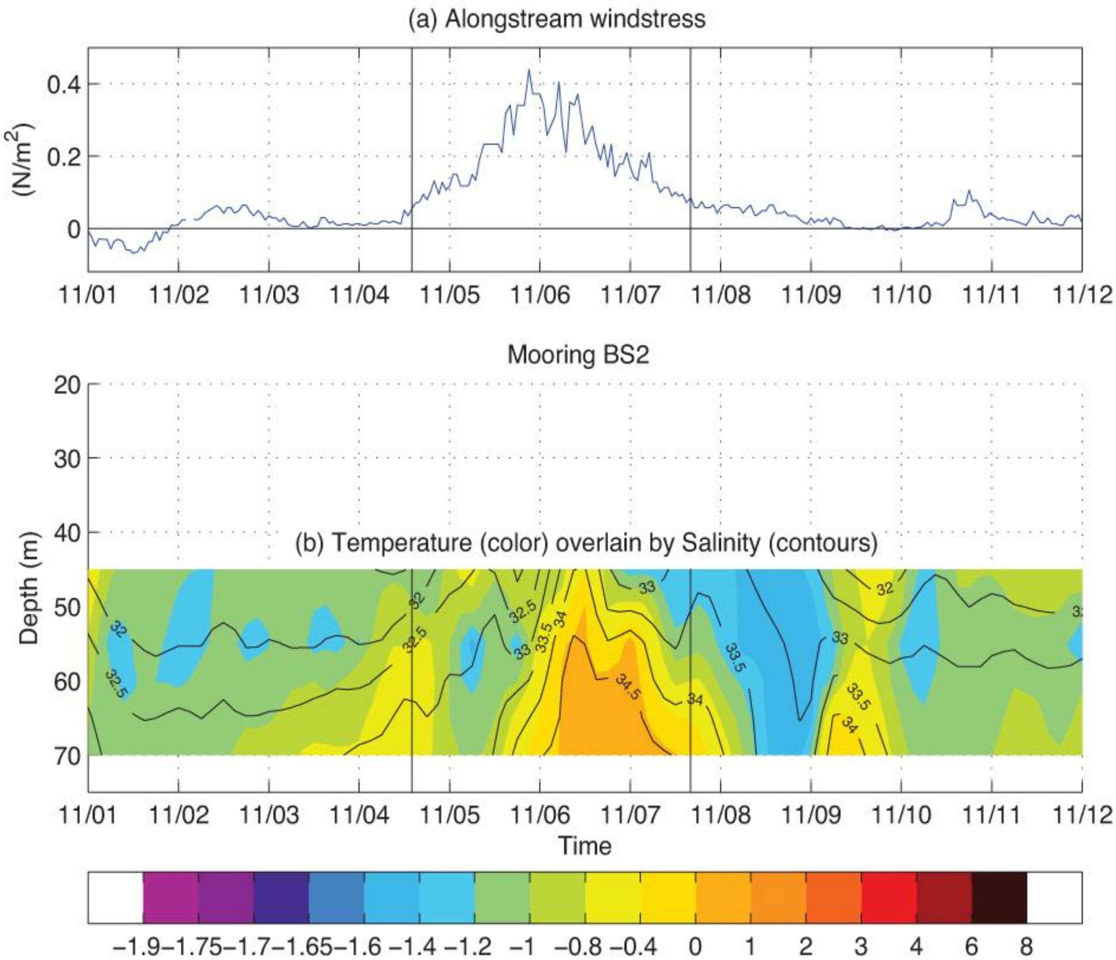

Figure 9: (a) Wind stress calculated from the Barrow meteorological timeseries for the first 12 days of November 2002. The vertical lines denote the period of the upwelling event. (b) Potential temperature (color, °C) overlain by salinity (contours) from the CTD profiler at mooring BS2 for the same period.

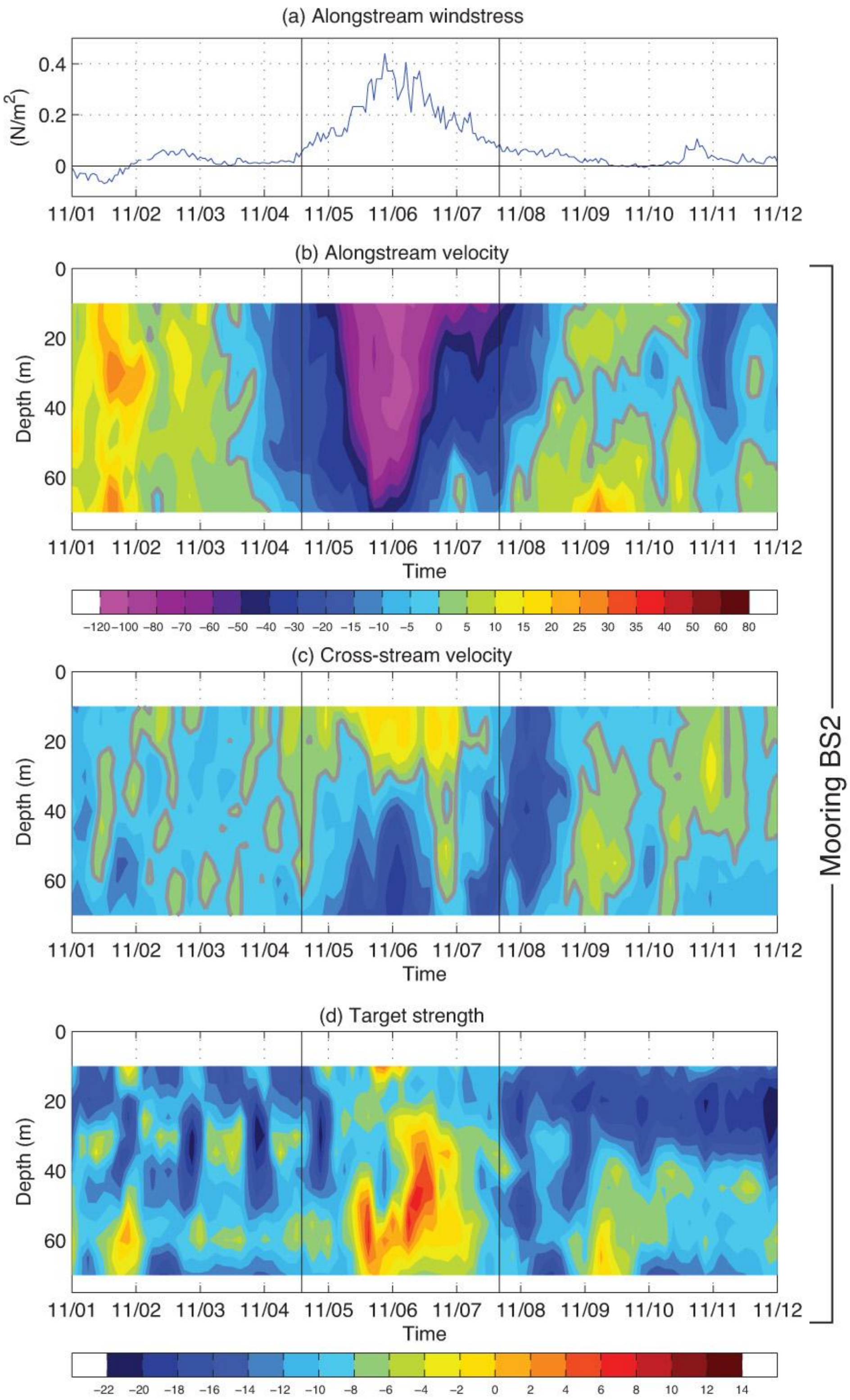

Figure 10: (a) Wind stress calculated from the Barrow meteorological timeseries for the first 12 days of November 2002. The vertical lines denote the period of the upwelling event. The remaining panels show variables measured from the ADCP at mooring BS2 for the same period. The units of velocity are cm s^{-1}.

would be expected if the whales are responding to the introduction of prey onto the shelf. Fig. 12c shows the salinity difference between the two composites, which indicates the presence of anomalously salty water on the upper-slope and outer-shelf – i.e., the basin water containing the elevated zooplankton (recall that we are unable make a vertical section of relative target strength).

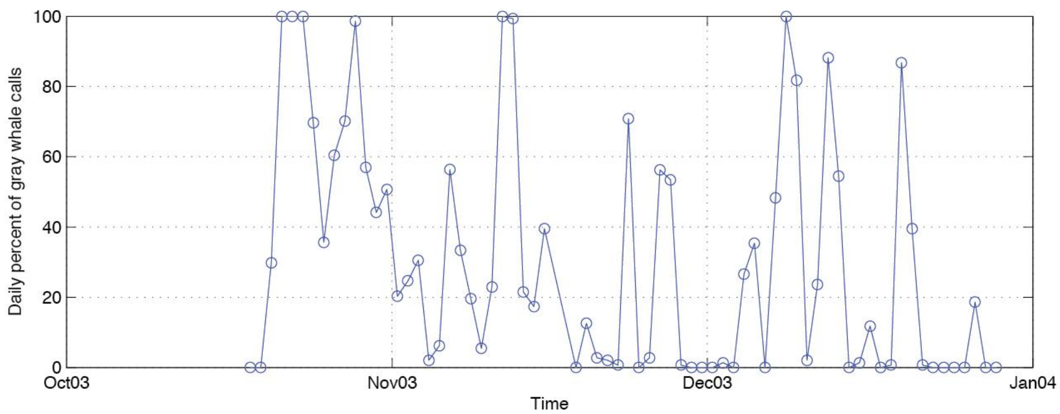

Figure 11: Daily percent of gray whale occurrence from the ARP on the upper continental slope (see Fig. 2 for the location of the instrument).

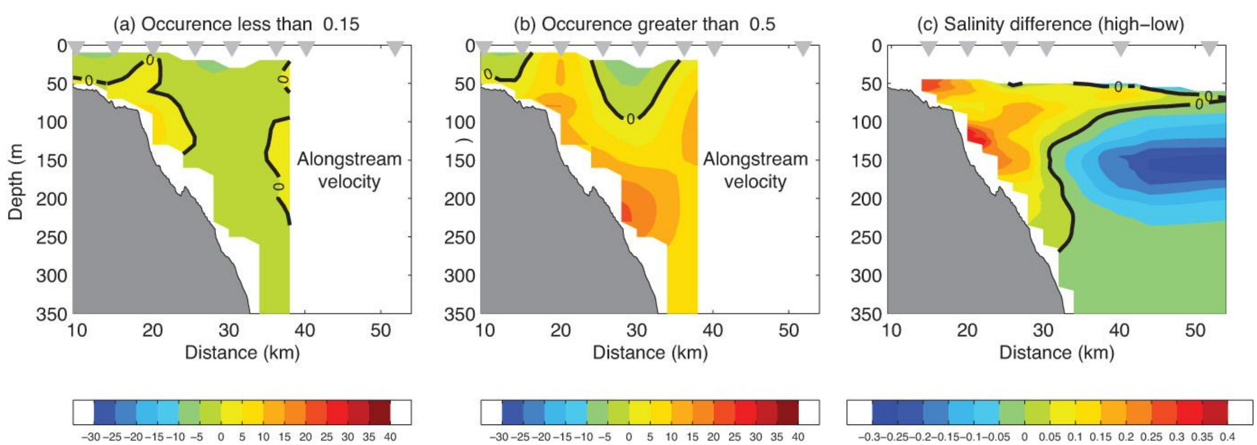

Figure 12: (a) Composite vertical section of alongstream velocity (cm s^{-1}) for periods when the gray whale occurrence was less than 15%. (b) Same as (a) except for periods when the gray whale occurrence was greater than 50%. (c) The difference in salinity between the two composites (high occurrence minus low occurrence). The mooring locations are marked along the top.

As noted by Stafford et al. (2007), increased openings in the pack ice in recent years provide pathways for the gray whales to navigate during the fall and winter months. Inspection of the

AMSR-E ice concentration data for the period considered here indicates that the ice cover in the region from the inner shelf to the mooring array was quite variable and rarely reached 100%. To quantify this, we considered the area within the box in Fig. 2 and computed the fraction of the box that contained ice concentration > 90% for each day. The assumption here is that gray whales would have difficulty navigating through > 90% concentrated ice. The mean fraction of such impenetrable ice for the boxed region was 0.65±0.40 over the time period, and ranged from 0 to 1. This suggests that gray whales would be able to frequent this region regularly. There were only three periods of impenetrable ice within the box (i.e. fractions close to 1), lasting 6 days, 4 days, and 7 days, respectively.

Figure 13 compares the percent occurrence of gray whales, computed from the ARP, and the target strength measured at mooring BS2 on the outer shelf (the target strength had a period of no data return early in the record). This demonstrates a clear relationship between the presence of gray whales and the availability of zooplankton. The particularly large values of target strength at the beginning of the record were associated with a pronounced extended period of upwelling that began on 18 October, i.e. just when the percent whale occurrence climbed to 100% at the

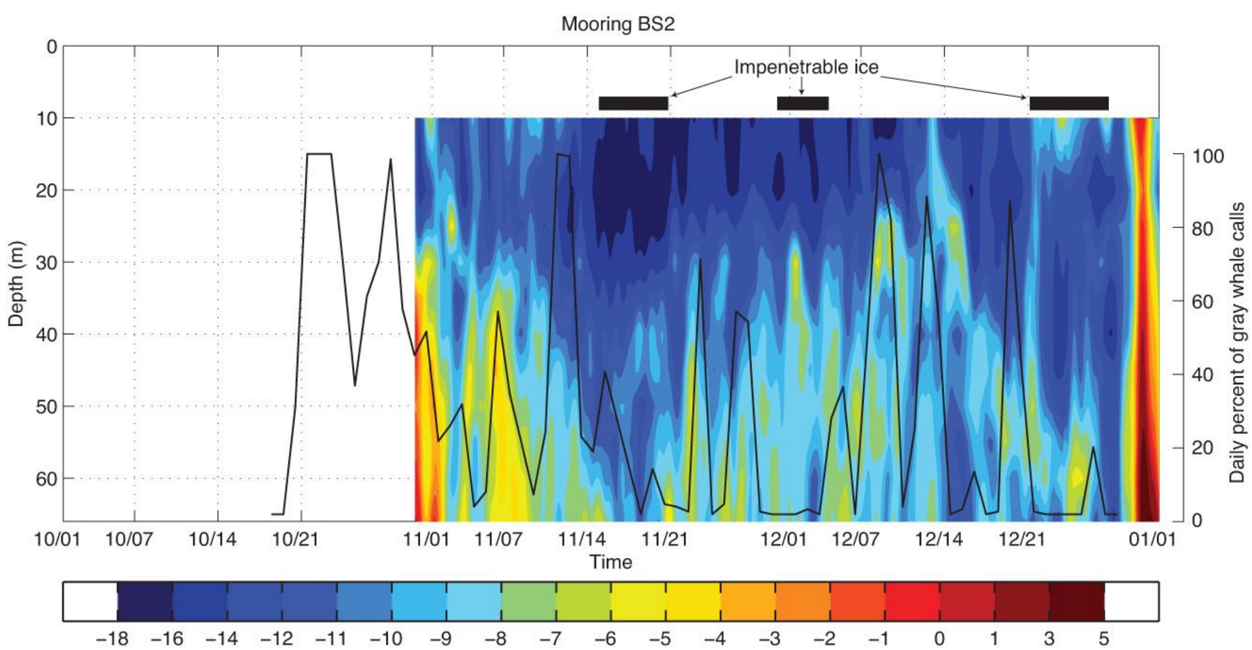

Figure 13: Target strength (color) from mooring BS2 in autumn 2003, in relation to gray whale occurrence (black curve). The three periods of impenetrable ice cover are indicated by the thick black bars (see text).

beginning of the ARP record. This implies that the high whale occurrence in the latter half of October was associated with large values of target strength resulting from this upwelling (which would have been captured had the ADCP returned good data during that time).

Over the rest of the record one sees that the peaks in whale occurrence are generally associated with enhanced target strength. However, the opposite is not always true. For instance, at the beginning of December there was reasonably high target strength, yet the whale occurrence was near-zero. This can be explained by the fact that there was impenetrable ice in the region during this time (denoted by the thick black bars in Fig. 13). Another example of this is near 21 November. On the other hand, during the last period of impenetrable ice there was enhanced target strength associated with increased whale presence (which could simply mean that our ice criterion is not perfect). The sole exception to the whale-zooplankton relationship occurred around 17 December when there was a large value of target strength without any whale activity despite the fact that the ice was not impenetrable. One must keep in mind, however, that the availability of prey is not a sufficient condition for whales to be present in the area.

6. Summary

This study used physical data from a mooring array across the Beaufort shelf/slope to shed light on the variability of gray whale occurrence measured in this region during autumn. The goal was to determine if the whales respond to the flux of zooplankton onto the shelf during wind-driven upwelling events.

When winds are light, the Beaufort shelfbreak jet advects Pacific water to the east with different seasonal configurations. In spring the current is bottom-intensified and transports primarily Pacific-origin winter water, while in summer it is surface-intensified when Alaskan coastal water is present. During winter it becomes bottom-intensified again and the dominant water mass is remnant winter water. During periods of enhanced easterly winds, which are common in the fall, the shelfbreak jet reverses to the west and upwelling commences, bringing water from the adjacent basin onto the shelf. As the easterly winds relax, an eastward-flowing rebound jet is temporarily established that extends into the Atlantic layer. This sequence of events is ubiquitous to the Alaskan Beaufort slope and occurs during all ice conditions, provided the pack ice is mobile.

The target strength computed using the ADCP backscatter can be used as a proxy for zooplankton in the water column because the backscatter signal shows diel variability coordinated with the daily light cycle, consistent with the diel vertical migration of euphausiids and large copepods known to be present in this region. In autumn the diurnal signal is largest in the depth range of 30-40 m. This is likely because the zooplankton are congregated there due to the strong stratification at the base of the mixed layer. Over the course of the fall this signal weakens and gradually becomes deeper, likely due to the deepening of the mixed layer. During upwelling events in autumn, the secondary circulation advects large amounts of zooplankton onto the shelf. These zooplankton, originating from depth, had likely begun their over-wintering period in the Canada Basin. The upwelling makes them available as prey to gray whales on the shelf.

The passive acoustic data collected near the mooring array revealed the presence of gray whales throughout the fall and early-winter. Compositing the periods when the daily percent occurrence was less than 15%, versus those times when it was greater than 50%, revealed a clear pattern. Namely, when the Beaufort shelfbreak jet was in its normal configuration, with light winds, the whales were sparse. By contrast, at the end of upwelling events when the basin water was still on the outer-shelf and upper-slope – and the rebound jet was present – larger numbers of gray whales resided in the area. Comparison of the timeseries of target strength and gray whale occurrence shows that peaks in whale occurrence are generally associated with enhanced levels of zooplankton, provided the ice cover does not prohibit the mobility of the whales. Overall, our results suggest an important predator-prey relationship for gray whales and zooplankton associated with autumn upwelling on the Beaufort slope.

Acknowledgements

The authors thank the officers and crew of the USCGC *Healy*, along with technicians John Kemp, Jim Ryder, and Sean Wiggins, for the successful deployment and recovery of the instrumentation used in this study. Gratia Montgomery helped make the project possible. The fieldwork was funded by contract N00014-02-1-0317 of the Office of Naval Research. Support for the analysis was provided by the National Science Foundation under grant PLR-1303617 (RP and DT).

References

Aagaard, K., 1984. The Beaufort Undercurrent. The Alaskan Beaufort Sea: Ecosystems and Environments. Academic Press, 47-71.

Ashjian, C. J, R. G. Campbell, H. E. Welch, M. Butler, and D, Keuren, 2003. Annual cycle in abundance, distribution, and size in relation to hydrography of important copepod species in the western Arctic Ocean. *Deep Sea Research*, **50**, no. 10-11, pp. 1235-1261.

Ashjian, C. J., S. M. Gallager, S. Plourde, 2005. Transport of plankton and particles between the Chukchi and Beaufort Seas during summer 2002, described using a Video Plankton Recorder. *Deep-Sea Research II,* **52**: 3259-3280.

Ashjian, C.J., S.R. Braund, R.G. Campbell, J.C. George, J. Kruse, W. Maslowski, S.E. Moore, C.R. Nicolson, S.R. Okkonen, B.F. Sherr, E.B. Sherr and Y. Spitz. 2010. Climate variability, oceanography, bowhead whale distribution and Inupiat subsistence whaling near Barrow, Alaska. *Arctic* **63**(2): 179-194.

Berg, J., Cottier, F., Last, K.S., Varpe, Ø., Leu, E., Søreide, J., Eiane, K., Falk-Petersen, S., Willis, K., Nygård, H., VOgedes, D., Grifiths, C., Johnsen, G., Lorentzen, D., Brierley, A.S. 2008. Diel vertical migration of Arctic zooplankton during the polar night. *Biology Letters* doi:10.1098/rsbl.2008.0484

Brugler, E. T., R. S. Pickart, G. W. K. Moore, S. Roberts, T. J. Weingartner, and H. Statscewich, 2014. Seasonal to Interannual Variability of the Pacific Water Boundary Current in the Beaufort Sea. *Progress in Oceanography,* **127**, 1-20, http://dx.doi.org/10.1016/j.pocean.2014.05.002

Clarke, J.T., Kennedy A.S., Ferguson, M.C., 2016. Bowhead and gray whale distributions, sighting rates and habitat associations in the eastern Chukchi Sea, Summer and Fall 2009-15, with a retrospective comparison to 1982-91. *Arctic* **69**(4): 359-377.

Corlett, W. B. and R. S. Pickart, 2017. The Chukchi slope current, *Progress in Oceanography,* **153**, 50-56, http://dx.doi.org/10.1016/j.pocean.2017.04.005.

Cottier, F. R., Tarling, G. A., Wold, A. Falk-Petersen, S. 2006 Unsynchronised and synchronised vertical migration of zooplankton in a high Arctic fjord. *Limnology and Oceanography*, **51**, 2586–2599.

Coyle, K.O. Coyle and A.I. Pinchuk, 2002. Climate-related differences in zooplankton density and growth on the inner shelf of the southeastern Bering Sea. *Progress in Oceanography*, **55**, 177-194.

Falk-Petersen, S., Leu, E., Berge, J., Kwasniewski, S., Nygård, H., Røstad, A., Keskinen, E., Thormar, J., von Quillfeldt, C., Wold, A., Gulliksen, B. 2008. Vertical migration in high Arctic waters during autumn 2004. *Deep-Sea Research II* **55**: 2275-2284.

Falk-Petersen, S., Mayzaud, ., Kattner, G., Sargent, J.R. 2009. Lipids and life strategy of Arctic Calanus. *Marine Biology Research* **5**: 18-39.

Hamilton, J.M., Collins, K., Prinsenberg, S.J. 2013. Links between ocean properties, ice cover, and plankton dynamics on interannual time scales in the Canadian Arctic Archipelago. *Journal of Geophysical Research Oceans* **118**, 5625-5630. doi:10.1002/jgrc.20382

Hauser, D. D.W., Laidre, K.L., Stern, H.L., Moore, S.E., Suydam, R.S., Richard, P.R., 2017. Habitat selection by two beluga whale populations in the Chukchi and Beaufort Seas. PLoS ONE 12(2):e0172755. doi: 10.1371/journalpone.0172755.

Hopcroft, R.R., C. Clarke, A.G. Byrd, and A.I. Pinchuk, 2005. The paradox of *Metridia* spp. egg production rates: a new technique and measurements from the coastal Gulf of Alaska. *Marine Ecology Progress. Series.* **286**, pp. 193-201.

Lane, P. V.Z., D. Sorarrain-Pilz, S. L. Smith, and L. Llinás, 2006. Zooplankton Data Report: Distribution of zooplankton in the Western Arctic during summer 2002. *RSMAS Technical Report 2006-01*, 130 pp.

Lane, P. V.Z., L. Llinás, S. L. Smith, D. Pilz. 2008. Distribution of zooplankton in the Western Arctic during summer 2002: Hydrographic habitats and implications for food chain dynamics. *Journal of Marine Systems* **70**: 97-133.

Large, W.G. and S. Pond, 1981. Open Ocean Momentum Flux Measurements in Moderate to Strong Winds. *Journal of Physical Oceanography*, **11**, 324-336

Lin, P., R. S. Pickart, K. M. Strafford, G. W. K. Moore, D. J. Torres, F. Bahr, and J. Hu, 2016. Seasonal Variation of the Beaufort Shelfbreak Jet and its Relationship to Arctic Cetacean Occurrence. *Journal of Physical of Geophysical Research*, **121**, doi:10.1002/2016JC011890.

Lin, P., R. S. Pickart, G. W. K. Moore, M. A. Spall, and J. Hu. Characteristics and dynamics of wind-driven upwelling in the Alaskan Beaufort Sea based on six years of mooring data. *Deep-Sea Research II*, submitted. http://rpickart.whoi.edu/wp-content/uploads/sites/53/2016/12/Lin_etal_DSR_submit.pdf

Llinas, L., R. S. Pickart, J. T. Mathis, and S. L. Smith, 2009. Zooplankton inside an Arctic Ocean cold-core eddy: Probable origin and fate. *Deep-Sea Research II*, **56**, 1290-1304.

Mathis, J. T., R. S. Pickart, and 14 co-authors, 2012. Storm-Induced Upwelling of High pCO2 Waters onto the Continental Shelf of the Western Arctic Ocean and Implications for Carbonate Mineral Saturation States. *Geophysical Research Letters*, **39**, L07606, doi:10.1029/2012GL051574.

MacIntyre, K. Q. and K .M. Stafford, 2011. Year-round passive acoustic monitoring of bearded seal vocalizations at two locations in the Beaufort Sea. Alaska Marine Science Symposium, 17-21 January 2011, Anchorage AK.

Moore, S. E., D. P. DeMaster, D. P., and P. K. Dayton, 2000. Cetacean Habitat Selection in the Alaskan Arctic during Summer and Autumn. *Arctic.* Vol. **53**, no. 4, pp. 432-447.

Moore, S.E., J.C. George, G. Sheffield, J. Bacon, C.J. Ashjian.2010. Bowhead whale distribution and feeding near Barrow, Alaska in late summer 2005-06. *Arctic* **63**(2)*:* 195-205

Moore, S. E., K. M. Stafford, H. Melling, C. Berchok, Ø. Wiig, K. M. Kovacs, C. Lydersen, and J. Richter-Menge, 2012. Comparing marine mammal acoustic habitats in Atlantic and Pacific sectors of the High Arctic: year-long records from Fram Strait and the Chukchi Plateau. *Polar Biology*, **35**, 475–480.

Nerini, M. 1984. A review of gray whale feeding ecology. Pp. 423-448 In The Gray Whale, *Eschrichtius robustus*. M.L. Jones, S.L. Swartz, S. Leatherwood (eds). Academic Press, Inc. San Diego.

Nikolopoulos, A., R. S. Pickart, P. S. Fratantoni, K. Shimada, D. J. Torres, and E. P. Jones, 2009. The western Arctic boundary current at 152°W: Structure, variability, and transport. *Deep-Sea Research II*, **56**, 1164-1181.

Okkonen S.R., C. Ashjian, R. Campbell, J. Clarke, S. E. Moore, and K. Taylor, 2011. Satellite observations of circulation features associated with a bowhead whale feeding "hotspot" near Barrow, Alaska. *Remote Sensing of Environment* **115**:2168–2174.

Okkonen, S.R., Clarke, J.T., Potter, R.A. 2017. Relationships among high river discharges, upwelling events, and bowhead whale (*Balaena mysticetus*) occurrence in the central Alaskan Beaufort Sea. *Deep-Sea Research II*, in press.

Pacini, A., R. Pickart, K. Moore, C. Nobre, F. Bahr, K. Vage, and K. Arrigo, 2017: Characteristics and transformation of Pacific winter water on the Chukchi Sea shelf in late-spring. *Deep-Sea Research II*, Submitted. http://rpickart.whoi.edu/pickart/wp-content/uploads/sites/53/2017/03/DSR2_2017_17_Original_V0.pdf

Pawlowicz, R., R. Beardsley, and S. Lentz, 2002. Classical tidal harmonic analysis including error estimates in MATLAB using T_TIDE. *Computers and Geosciences*, **28**, 929-937.

Pickart, R. S., G. W. K. Moore, D. J. Torres, P. S. Fratantoni, R. A. Goldsmith, and J. Yang, 2009. Upwelling on the continental slope of the Alaskan Beaufort Sea: Storms, ice, and oceanographic response. *Journal of Geophysical Research*, **114**, C00A13, doi:10.1029/2008JC005009.

Pickart, R. S., M. A. Spall, G.W.K. Moore, T. J. Weingartner, R. A. Woodgate, K. Aagaard, and K. Shimada, 2011. Upwelling in the Alaskan Beaufort Sea: Atmospheric Forcing and local versus non-local response. *Progress in Oceanography*, doi:10.1016/j.pocean.2010.11.005.

Pickart, R. S., M. A. Spall, and J. T. Mathis, 2013a. Dynamics of upwelling in the Alaskan Beaufort Sea and associated shelf-basin fluxes. *Deep-Sea Research I*, **76**, 35-51.

Pickart, R. S., L. M. Schulze, G. W. K. Moore, M. A. Charette, K. R. Arrigo, G. van Dijken, and S. L. Danielson, 2013b. Long-term trends of upwelling and impacts on primary productivity in the Beaufort Sea. *Deep-Sea Research I*, **79**, 106-121.

Rosenfeld, L.K., 1987. Tidal band current variability over the northern California continental shelf. Ph.D. thesis, Woods Hole Oceanographic Institution/Massachusetts Institute of Technology Joint Program in Oceanography and Oceanographic Engineering, WHOI-87-11, 237 pp.

Schulze, L. M., and R. S. Pickart, 2012. Seasonal variation of upwelling in the Alaskan Beaufort Sea: Impact of sea ice cover, *Journal of Geophysical research- Oceans*, **117**, C06022, doi: 10.1029/2012JC007985

Smoot, C.A., Hopcroft, R.R. 2017a. Depth-stratified community structure of Beaufort Sea slope zooplankton and its relations to water masses. *Journal of Plankton Research* **39**(1): 79-91, doi:10.1093/plankt/fbw087

Smoot, C.A., Hopcroft, R.R. 2017b. Cross-shelf gradients of epipelagic zooplankton communities of the Beaufort Sea and the influence of localized hydrographic features. *Journal of Plankton Research* **39**(1): 65-78. doi:10.1093/plankt/fbw080.

Spall, M. A., R. S. Pickart, P. S. Fratantoni, and A. J. Plueddemann, 2008. Western Arctic shelfbreak eddies: Formation and transport. *Journal of Physical Oceanography*, **38**, 1644-1668.

Spreen, G., L. Kaleschke, and G. Heygster, 2008. Sea ice remote sensing using AMSR-E 89 GHz channels, *Journal of Geophysical Research*, **113**, doi:10.1029/2005JC003384.

Stafford, K. M., S. E. Moore, M. Spillane, and S. Wiggins, 2007. Gray Whale Calls Recorded near Barrow, Alaska, throughout the Winter of 2003-04. *Arctic*, **60**, 167-172.

Stafford K. M., S. R. Okkonen, and J. T. Clarke, 2013. Correlation of a strong Alaska Coastal Current with the presence of beluga whales (Delphinapterus leucas) near Barrow, Alaska. *Marine Ecology Progress Series*. **474**:287-297.

Timmermans, M.-L., J. T. Toole, A. Proshutinsky, R. Krishfield, and A. Plueddemann, 2008. Eddies in the Canada Basin, Arctic Ocean, observed from ice-tethered profilers. *Journal of Physical Oceanography*, **38**, 133-145.

Urick, R.J., 1983. Principles of Underwater Sound, Third Edition, McGraw-Hill, New York.

Visbeck, M., 2002. Deep velocity profiling using lowered acoustic Doppler current profilers: Bottom track and inverse solutions. *Journal of Atmospheric and Oceanic Technology*, **19**, 794–807.

Von Appen, W-J., and R. S. Pickart, 2012. Two configurations of the Western Arctic shelfbreak current in summer. *Journal of Physical Oceanography*, **42**, 329-351. doi: 10.1175/JPO-D-11-026.1.

Wiggins, S., 2003. Autonomous Acoustic Recording Packages (ARPs) for long-term monitoring of whale sounds. *Marine Technology Society Journal*, **37**, 13-22.